AL-TR-1991-0045

(2)

A GRID-FREE METHOD FOR HIGH REYNOLDS NUMBER FLOW AROUND AN IMMERSED ELASTIC STRUCTURE

Lisa J. Fauci

Department of Mathematics
Tulane University
New Orleans, LA 70118

AEROSPACE MEDICINE DIRECTORATE
Brooks Air Force Base, TX 78235-5000

May 1991

Final Report for Period June 1988 – December 1990

Approved for public release, distribution is unlimited.

AIR FORCE SYSTEMS COMMAND
BROOKS AIR FORCE BASE, TEXAS 78235-5000

NOTICES

This effort was funded wholly through the In-House Laboratory Independent Research Program. The work was completed under contract with the Air Force Office of Scientific Research (AFOSR).

This report has been reviewed and is approved for publication.

SHERWOOD W. SAMN, Ph.D.
Project Scientist

JAMES R. HICKMAN, JR.
Colonel, USAF, MC, CFS

REPORT DOCUMENTATION PAGE

Form Approved
OMB No. 0704-0188

1. AGENCY USE ONLY (Leave blank)	2. REPORT DATE	3. REPORT TYPE AND DATES COVERED
	May 1991	Final June 1988 - Dec 1990

4. TITLE AND SUBTITLE
A Grid-free Method for High Reynolds Number Flow Around an Immersed Elastic Structure

5. FUNDING NUMBERS
PE - 61101F
PR - 7755
TA - 27
WU - 16

6. AUTHOR(S)
Lisa J. Fauci

7. PERFORMING ORGANIZATION NAME(S) AND ADDRESS(ES)
Tulane University
Department of Mathematics
New Orleans, LA 70118

8. PERFORMING ORGANIZATION REPORT NUMBER
AFOSR-89-0295

9. SPONSORING / MONITORING AGENCY NAME(S) AND ADDRESS(ES)
Armstrong Laboratory
Aerospace Medicine Directorate
Brooks Air Force Base, TX 78235-5000

10. SPONSORING / MONITORING AGENCY REPORT NUMBER
AL-TR-1991-0045

11. SUPPLEMENTARY NOTES
Armstrong Laboratory Technical Monitor: Dr. Sherwood W. Samn, (512) 536-3232
This effort was funded wholly through the In-House Laboratory Independent Research Program. The work was completed under contract with the Air Force Office of Scientific Research (AFOSR).

12a. DISTRIBUTION / AVAILABILITY STATEMENT
Approved for public release; distribution is unlimited.

12b. DISTRIBUTION CODE

13. ABSTRACT *(Maximum 200 words)*

Finite difference schemes do not perform well in simulations of high Reynolds number flow because a restrictive number of grid points must be used to resolve boundary layers. In this report we present a grid-free numerical method which may be used to calculate flows around an immersed elastic structure. Numerical results are presented in 2 simple cases: flow past a circular cylinder and flow past a flat plate. The boundary motion is specified and is not time dependent. However, this algorithm can be used to simulate more complicated, time dependent problems in biological fluid mechanics.

14. SUBJECT TERMS
Vortex method; Immersed boundary; Flow past cylinder; Numerical methods; High Reynolds number

15. NUMBER OF PAGES
30

16. PRICE CODE

17. SECURITY CLASSIFICATION OF REPORT	18. SECURITY CLASSIFICATION OF THIS PAGE	19. SECURITY CLASSIFICATION OF ABSTRACT	20. LIMITATION OF ABSTRACT
Unclassified	Unclassified	Unclassified	UL

TABLE OF CONTENTS

List of Figures

A GRID-FREE METHOD FOR HIGH REYNOLDS NUMBER FLOW AROUND AN IMMERSED ELASTIC STRUCTURE

INTRODUCTION

This report is concerned with the computational modeling of problems in biological fluid mechanics. Typically, these problems involve the study of flow about highly flexible, moving boundaries; for instance, distensible vessels, moving heart walls, and valves. The fluid along with the boundary constitutes a coupled mechanical system in the sense that the motion of the boundary is determined by that of the fluid, but at the same time the boundary exerts force on the fluid and alters its motion. With the advent of supercomputers, many of these problems which were previously intractable, can now be successfully analyzed.

An innovative computational approach, the *immersed boundary technique*, was introduced by Peskin [18] to model 2-dimensional blood flow in the left heart. Recently, this technique has been advanced to study other biofluiddynamic problems such as platelet aggregation [11], aquatic animal locomotion [8][10], peristaltic pumping of solid particles [9], fluid flow in the inner ear [4], and 3-dimensional blood flow in the heart [19][20]. This numerical method solves the full incompressible Navier-Stokes equations in a domain of fluid within which a massless, neutrally buoyant elastic boundary undergoing time dependent movements is immersed.

The Navier-Stokes equations have been solved using Chorin's finite difference scheme [6]. Theoretically, this scheme imposes no restriction on the Reynolds number of the flow to be modelled. (The Reynolds number is a nondimensional quantity which measures the ratio of inertial forces to viscous forces.) However, the higher the Reynolds number, the smaller the grid spacing and time step must be to ensure stability of the calculations. To model high Reynolds number flow (as in the heart), the amounts of computer time and memory needed become prohibitive and impractical.

Within the finite difference framework, we have adapted the second order projection method recently introduced by Bell, Colella, and Glaz [3] for the solution to the Navier-Stokes equations. Our results indicate that flows with higher Reynolds numbers can be modelled more stably with this code than with Chorin's scheme using the same number of grid points and the same time step. We have tested this scheme on a problem of flow past a tethered cylinder and the results have exhibited the expected phenomena of flow separation and vortex shedding. The cylinder is modelled as an immersed boundary. Samn [22] has tested the projection method on problems with a non-zero force density, as is the case of

immersed boundary calculations, in a class of problems where exact solutions are known. For moderately high Reynolds numbers, this projection method is quite promising.

For much higher Reynolds numbers, a grid-free vortex method combined with the immersed boundary technique may be more appropriate. An effort in this direction was made by McCracken and Peskin [17] in 1980. This effort was a hybrid method which represented vorticity both on a grid and as free-moving vortex elements. In light of the advances made in vortex methods and the incredible growth of computing power since then, a totally grid-free vortex method for 2-dimensional flow is now being implemented and tested. This report will describe the current status of this algorithm.

IMMERSED BOUNDARY TECHNIQUE

The flow of a viscous, incompressible fluid is governed by the incompressible Navier Stokes equations:

$$\begin{aligned} \rho\left[\frac{\partial \mathbf{u}}{\partial t} + \mathbf{u}\cdot\nabla\mathbf{u}\right] &= -\nabla p + \mu\Delta\mathbf{u} + \mathbf{F}(\mathbf{x},t) \\ \nabla\cdot\mathbf{u} &= 0 \end{aligned} \tag{1}$$

Here ρ = density, μ = viscosity, $\mathbf{u} = (u,v)$ = velocity, p = pressure, and $\mathbf{F}(\mathbf{x},t)$ is the external force per unit volume applied to the fluid. This external force field represents the force of the elastic boundary on the fluid. It is a delta-function layer of force which is zero away from the immersed boundary $\mathbf{X}(s,t)$. This representation will be the basis of the computational model.

Since the immersed boundary is taken to be elastic and massless, the density per unit length of the boundary force $\mathbf{f}(s,t)$ at a material point is determined by the boundary configuration at time t. This elastic force is transmitted directly to the fluid because the boundary is massless. This follows from Newton's second law for force balance at a boundary point: the force of the fluid on the boundary point and the elastic force on the boundary point must add up to zero. Therefore, the force of the boundary point on the fluid is equal to the elastic force on that point. The external force field is then:

$$\mathbf{F}(\mathbf{x},t) = \int \mathbf{f}(s,t)\delta(\mathbf{x} - \mathbf{X}(s,t))ds \tag{2}$$

Here the integration is over the immersed boundary, and δ is the 2-dimensional delta-function.

Since the fluid is viscous, the velocity field is continuous across the boundary. This implies that the velocity of a material point of the immersed boundary must be equal to the velocity of the fluid at that point:

$$\frac{\partial \mathbf{X}(s,t)}{\partial t} = \mathbf{u}(\mathbf{X}(s,t),t) = \int \mathbf{u}(\mathbf{x},t)\delta(\mathbf{x} - \mathbf{X}(s,t))d\mathbf{x} \tag{3}$$

Here the integration is over the entire fluid domain. This integral representation is not singular since the 2-dimensional delta function is integrated over both space dimensions.

The crucial feature of this model is that the immersed boundary is not our computational boundary in the Navier-Stokes solver (whether we are using finite differences or vortex methods). The boundary is a singular force field which alters the driving force in the fluid dynamic equations.

Algorithm

Given the fluid velocity field $\mathbf{u}^n$ and the configuration of the elastic boundaries $\mathbf{X}^n$ at time step n:

1) Calculate the force density $\mathbf{f}^n$ from the configuration $\mathbf{X}^n$.

2) Use $\mathbf{f}^n$ to determine the external force on the fluid: $\mathbf{F}^n$.

3) Solve the Navier-Stokes equations for $\mathbf{u}^{n+1}$.

4) Move the elastic boundary at the local fluid velocity to get $\mathbf{X}^{n+1}$.

Within the finite difference framework, step (3) has been solved using Chorin's finite difference method. Steps (2) and (4) involve the use of discrete delta functions which communicate information between the grid and the immersed boundary points (which do not coincide with grid points). We refer the reader to reference [18] for details.

Derivation of Force Density

We will first model a *stationary* immersed boundary to illustrate our choice of force density. Consider a boundary made up of a continuum of material points $\mathbf{X}(s,t) = (x(s,t), y(s,t))$ which is in equilibrium when its material points coincide with the tether points $\mathbf{X}^*(s) = (x^*(s), y^*(s))$. We imagine there is a spring connecting $\mathbf{X}(s,t)$ to $\mathbf{X}^*(s)$ and that it has resting length zero.

The elastic force acting on a point $\mathbf{X}(s,t)$ is then:

$$\mathbf{f}(s,t)ds = -S[\mathbf{X}(s,t) - \mathbf{X}^*(s)]ds \tag{4}$$

S is the stiffness constant of the spring, and it may be thought of in 2 ways:

1) A physical parameter which reflects material properties of the elastic boundary.

2) A numerical parameter which should be made as large as possible to strictly enforce the equilibrium position of the elastic boundary.

This representation of the force density assumes that we know a priori the equilibrium position of the boundary in fixed space. This representation will be useful in our test examples where our immersed boundary will be either a fixed cylinder or a fixed flat plate. However, in most applications, the motion which we choose to specify is the time-dependent configuration of the boundary with respect to itself. The actual displacement relative to spatial coordinates is not preset, but is determined by the equations of motion. For instance, we can choose forces at a boundary point due to the rest of the boundary as:

1) Spring-like forces which asks that the 'links' between successive points resist compression or expansion from a given arc length.

2) Bending-resistant forces which asks that the angle formed by neighboring links be a given function which changes with position and time.

We refer the reader to references [10][18] for more details on how different boundary configurations can be enforced by the proper choice of force density functions.

VORTEX METHOD

In this section, we will outline Chorin's vortex method [7], a grid-free scheme which represents the fluid field by a discrete collection of vortex elements.

Inviscid, incompressible flow in 2 dimensions in the absence of external forces is governed by the Euler equations:

$$\frac{D\mathbf{u}}{Dt} = -\nabla p \tag{5}$$

$$\nabla \cdot \mathbf{u} = 0 \tag{6}$$

The first term in equation (5) is the total derivative. We introduce the vorticity $\omega = \nabla \times \mathbf{u} \cdot (0,0,1) \quad v_x \quad u_y$. Taking curl of equation (5) gives:

$$\frac{D\omega}{Dt} = 0 \tag{7}$$

The vorticity acts as 'particles' which move with the fluid. It is, therefore, natural to model vorticity by a discrete collection of vortex elements around which the vorticity of the fluid is concentrated. The velocity can be recovered from the configuration and strengths of the vortex elements using a discrete form of the Biot-Savart law.

Since this flow is inviscid, there is no mechanism for creation or destruction of vorticity (Kelvin's circulation theorem). The vorticity is represented by a sum of m point vortices, the i th one centered at point $\mathbf{x}_i$ with strength κ_i:

$$\omega = \sum_{i=1}^{m} \omega_i = \sum_{i=1}^{m} \kappa_i \delta(\mathbf{x} - \mathbf{x}_i) \tag{8}$$

Here δ is the Dirac delta function.

The incompressibility condition implies the existence of a stream function $\psi(x, y)$ such that:

$$\psi_y = u \tag{9}$$
$$\psi_x = -v \tag{10}$$

The relation between the stream function and the vorticity is therefore:

$$\Delta\psi = -\omega \tag{11}$$

Using the representation (8) of vorticity, equation (11) can be solved explicitly (in the whole plane) by the formula:

$$\psi(\mathbf{x}) = \sum_{i=1}^{m} \frac{\kappa_i}{2\pi} log|\mathbf{x} - \mathbf{x}_i| \tag{12}$$

The velocity can be calculated directly from the stream function:

$$\mathbf{u}_x(\mathbf{x}) = \sum_{i=1}^{m} \frac{\kappa_i}{2\pi} \frac{(-(y - y_i), (x - x_i))}{|\mathbf{x} - \mathbf{x}_i|^2} \tag{13}$$

This formula, unfortunately, is infinite at each of the vortex centers $\mathbf{x}_i$. This problem is overcome by the convention that the induced self velocity of a point vortex, in the absence of boundaries, is zero. The convection equation for vorticity (7) is solved by moving the point vortices at the local fluid velocity:

$$\frac{d\mathbf{x}_i}{dt} = \sum_{j \neq i} \frac{\kappa_j}{2\pi} \frac{(-(y_i - y_j), (x_i - x_j))}{|\mathbf{x}_i - \mathbf{x}_j|^2} \tag{14}$$

Notice that this Lagrangian description of the vorticity field overcomes the difficulty of the nonlinearity in the convection equation.

Thus far we've been considering an unbounded domain. In a region of fluid with stationary boundary $\partial\Omega$, the boundary condition which must be satisfied in this inviscid flow is:

$$\mathbf{u} \cdot \mathbf{n} = 0 \quad on \quad \partial\Omega \tag{15}$$

where $\mathbf{n}$ is the normal to the boundary. (If the boundary is moving at velocity $\mathbf{V}$, the condition becomes $\mathbf{u} \cdot \mathbf{n} = \mathbf{V} \cdot \mathbf{n}$.) This condition can be satisfied by adding a potential flow to the velocity in (13):

$$\mathbf{u} = \mathbf{u}_\omega + \nabla\phi \tag{16}$$

Taking divergence of this expression, we get:

$$\Delta\phi = 0 \tag{17}$$

$$\partial_{\mathbf{n}}\phi = -\mathbf{u}_\omega \cdot \mathbf{n} \tag{18}$$

A Neumann problem must be solved for ϕ. Depending upon the geometry of the problem, this can be done through the use of conformal mapping where proper image vortices are introduced [12][21].

The vortex method for incompressible, viscous flow is based on these ideas. The major difference between the Navier-Stokes equations and the Euler equations, besides the diffusion term, is the role of boundaries. The condition at a stationary boundary is now the no-slip condition:

$$\mathbf{u} = 0 \quad on \quad \partial\Omega \tag{19}$$

Not only is the normal velocity zero, but also the tangential velocity. Also, unlike inviscid flow, vorticity can be created.

Consider flow past an infinite flat plate with uniform velocity $(U, 0)$ at infinity. The solution of the inviscid equations is $\mathbf{u} = (U, 0)$ everywhere. However, in the viscous case, there must be zero velocity at the plate.

The transition region from the boundary to the uniform flow at infinity (the boundary layer) has thickness on the order of $1/\sqrt{R}$, where R = Reynolds number. Within this boundary layer, vorticity is created. For large Reynolds numbers, the boundary layer is quite small. Here, again, the inadequacy of finite difference schemes for large Reynolds number flow becomes evident. To resolve what is going on in the boundary layer, a minimum number of mesh points is needed within that region. This resolution leads to a prohibitively small mesh width and time step.

Vortex Method for Viscous Flow

The Navier-Stokes equations for 2-dimensional flow in stream function - vorticity formulation are :

$$\frac{D\omega}{Dt} = \frac{1}{R}\Delta\omega \tag{20}$$

$$\Delta\psi = -\omega \tag{21}$$

$$u = \psi_y \tag{22}$$

$$v = -\psi_x \tag{23}$$

As before, the vorticity field is represented by a discrete collection of vortex elements. These vortex elements will be moved both by convection and diffusion. In practice, it is necessary to spread the point vortices into 'vortex blobs'[12] because the velocity given by equation (13) becomes infinite as the vortex centers are approached. There are many choices for desingularizing this kernel which have been analyzed and implemented [2] [7]. We used the approximation suggested by Krasny [15]. Using a discretized version of the Biot-Savart law, the velocity field in an unbounded fluid induced by these modified point vortices is:

$$\mathbf{u}_\omega = \sum_{i=1}^{m} \frac{\kappa_i}{2\pi} \frac{(-(y - y_i), (x - x_i))}{|\mathbf{x} - \mathbf{x}_i|^2 + \sigma^2} \tag{24}$$

where σ is smoothing parameter.

The no-slip boundary condition on $\partial\Omega$ is split up into 2 parts:

$$\mathbf{u} \cdot \mathbf{n} = 0 \tag{25}$$

$$\mathbf{u} \cdot \tau = 0 \tag{26}$$

Here $\mathbf{n}$ is the normal vector and τ is the tangent vector to $\partial\Omega$. The first condition is satisfied by the introduction of a potential flow, as in equation (16). By definition, $\mathbf{u} \cdot \tau$ should be zero at the boundary (since $\mathbf{u} = 0$ on the boundary). However, $\mathbf{u} \cdot \tau$ will not, in general, be zero at the boundary. This fact implies the existence of a delta-function layer of vorticity at the boundary. The circulation per unit length of this vortex layer is $-\mathbf{u} \cdot \tau$. The second condition is, therefore, satisfied by the creation of vortex elements at the boundary with these strengths. (The boundary is partitioned into pieces of length Δs, and a modified point vortex of strength $-2[\mathbf{u} \cdot \tau]\Delta s$ is placed at its center. The factor of 2 accounts for elements which will immediately fall outside the boundary during a random walk, as explained later.) This numerical creation of vorticity at the boundary mimics what physically occurs.

The vortex algorithm for solution of the Navier-Stokes equations is as follows. Given the centers $\mathbf{x}_i$ and strengths κ_i of the vortex elements at time step n :

1. Satisfy the tangential boundary condition by creating new vortex elements at the boundary.

2. Move all of the vortex elements:

$$\mathbf{x}_i^{n+1} = \mathbf{x}_i^n + \Delta t(\mathbf{u}_\omega^n + \nabla\phi^n) + \eta_i \tag{27}$$

Here the η_i are independent Gaussian random variables with mean zero and variance $2\Delta t / R$. This random walk accounts for the diffusion term in the vorticity convection equation.

This algorithm is a fractional step algorithm which first solves the convection step, and then the diffusion. For discussion of convergence the reader is referred to Goodman [14].

GRID-FREE METHOD WITH IMMERSED BOUNDARY

The vortex method described earlier is grid-free, and thus the small mesh width restriction of finite difference schemes for large Reynolds numbers is circumvented. We have developed a vortex method to solve the coupled system of a viscous fluid and an immersed elastic boundary. Our treatment of the elastic boundary as a vorticity source is based on McCracken and Peskin [17].

The fluid only feels the presence of the immersed boundary as a singular distribution of external forces:

$$\mathbf{F}(\mathbf{x},t) = \int_B \mathbf{f}(s,t)\delta(\mathbf{x} - \mathbf{X}(s,t))ds \tag{28}$$

Here the integration is over the immersed boundary, and δ is the 2-dimensional delta function. We need to examine how this contributes to the evolution of the vorticity. Following McCracken and Peskin [17], we see that the curl of the external force acts as a source of vorticity:

$$\frac{D\omega}{Dt} = \frac{1}{R}\Delta\omega + (\nabla \times \mathbf{F}) \cdot \mathbf{k} \tag{29}$$

Here $\mathbf{k} = (0,0,1)$. We have:

$$(\nabla \times \mathbf{F}) \cdot \mathbf{k} = \int_B [\nabla \times (\delta(\mathbf{x} - \mathbf{X}(s,t))\ \mathbf{f}] \cdot \mathbf{k}\ ds \tag{30}$$

$$= \int_B \nabla\delta(\mathbf{x} - \mathbf{X}(s,t)) \cdot (f_2, -f_1)\ ds \tag{31}$$

where $\mathbf{f} = (f_1, f_2)$. The above integrand can be interpreted as a directional derivative. We discretize this integral as follows:

$$\sum \frac{\delta(\mathbf{x}^+ - \mathbf{X}(s,t)) - \delta(\mathbf{x}^- - \mathbf{X}(s,t))}{2h} |\mathbf{f}| \Delta s \tag{32}$$

where

$$\mathbf{x}^+ = \mathbf{x} + h\ \frac{(f_2, -f_1)}{|\mathbf{f}|} \tag{33}$$

$$\mathbf{x}^- = \mathbf{x} - h\ \frac{(f_2, -f_1)}{|\mathbf{f}|} \tag{34}$$

Here h is a small parameter.

Therefore, the immersed boundary acts a source of vortex dipoles with dipole moment:

$$(f_2, -f_1)\ \Delta s\ \Delta t \tag{35}$$

We multiply by Δt to get the amount of vorticity to be generated over one time step.

This dipole moment is not, in general, normal to the immersed boundary. McCracken and Peskin [17] split up the force density $\mathbf{f}$ into its tangential and normal components:

$$\mathbf{f} = f_\tau \tau + f_\eta \eta \tag{36}$$

where τ is the unit tangent to the immersed boundary curve, and η is the unit normal. It can be shown for a closed boundary, using integration by parts, that the normal component contributes a monopole layer of vorticity along the boundary with strength density:

$$\frac{d}{ds}\left[\frac{f_\eta(s)}{|\mathbf{X}'(s)|}\right] \tag{37}$$

If the immersed boundary curve is not closed, 2 additional vortex elements need to be introduced at the ends of the boundary due to the boundary terms in the integration by parts.

The tangential component of force still contributes a dipole layer as just described, but now this layer is oriented normal to the boundary. The process of splitting up the creation of vortex elements into a monopole layer and dipole layer oriented normal to the boundary adds more numerical stability to the calculations.

We now outline our basic vortex method in the plane within which there is an immersed boundary. The state of the system at time $t = n\Delta t$ is given by the configuration $\mathbf{X}_k^n$ of material points of the immersed boundary, and the discrete collection of modified point vortices centered at $\mathbf{x}_j^n$ with strengths κ_j^n. The basic algorithm is:

(1) Compute force density $\mathbf{f}_k^n$ using the current boundary configuration.

(2) Use step (1) to create new vortex elements at the boundary.

(3) Move each of the vortex elements in the velocity field induced by the other vortex elements plus a random walk to simulate diffusion.

(4) Compute the velocity at each of the points of the immersed boundary using equation (24). Move each of these points at this local fluid velocity.

This algorithm has the advantage of being grid free, and since it has no *real* boundaries, we needn't worry about the introduction of image vortices to satisfy the normal boundary condition discussed in the previous section.

Explicit evaluation of the force density at the current boundary configuration produces large instabilities. The reason for this condition is that the boundary is stiff and the forces are large enough to make the boundary overshoot equilibrium in one time step. We use the approximate-implicit method described by Peskin [18]. In general, when boundary points are coupled to each other through the forces, this approximate-implicit method requires the solution of a nonlinear optimization problem. However, in the examples addressed in this report, our immersed boundary points act as *independent* springs. Therefore, step (1) is performed very quickly.

In step (2), we either create 2 or 3 vortex elements per boundary point. This choice depends on whether we wish the dipole layer to be normal to the boundary - in which case we create both a dipole and a monopole layer of vorticity.

Steps (3) and (4) require the computation of velocities of the vortex elements and boundary points respectively using the current positions of vortex elements and their strengths. We use a second order Runge Kutta method to update the positions of the vortex elements and the boundary points.

COMPUTATIONAL RESULTS

Flow Past a Cylinder

Our first test problem will be flow past a circular cylinder. The cylinder is modelled by a collection of immersed boundary points which are tethered to fixed spatial positions by springs of resting length zero. We are deliberately choosing a test problem where the equilibrium position of the immersed boundary is known and is not time dependent. Flow past a cylinder has been well-studied since the qualitative features of the flow (such as vortex shedding) are Reynolds number dependent. For a detailed discussion of the simulation of flow past a cylinder using vortex methods, the reader is referred to Cheer [5]. Our simulations differ in that the cylinder is represented as a singular external force field in the fluid, and not a computational boundary.

We found that introducing the dipole layer normal to the cylinder made the calculations more stable. Therefore, at each time step, we create 3 vortex elements per boundary point. This layer is shown in Figure 1 for an immersed cylinder made up of 40 immersed boundary points. The cylinder has a diameter $d = .1\ cm$ and is placed in a uniform flow $U = 2\ cm/s$. We used a time step $\Delta t = .00025\ s$, and spacing between boundary points of $\Delta s = .1\pi/40\ cm$. The numerical parameter which represents the distance of the dipole vortex elements from the immersed boundary is $h = .8\Delta s$. The viscosity was chosen to be 10^{-8}. The smoothing parameter $\sigma = .75\Delta s$. The Reynolds number based upon the uniform flow velocity and diameter of the cylinder is therefore on the order of 10^7. The tethering stiffness constant used was 10^6.

Figures 2 and 3 show velocity fields of the flow about the cylinder at time $t = .0125\ s$. We show 2 space scales to emphasize the fact that because this is a grid-free method, the velocities may be calculated from the vortex element configuration at any spatial points by using equation (24). We are, therefore, able to resolve the boundary layer with a much finer degree of accuracy than if we were working on a fixed grid. Smoothing does take place, however, both in the representation of the vortex blob functions (parameter σ) and in the finiteness of the dipole layer (parameter h).

Stagnation points at the upstream and downstream centerline of the cylinder can be seen in Figures 2 and 3. The magnitude of the velocity vectors at the top and bottom of the cylinder are larger than the free stream velocity, as is to be expected. The flowfield within the cylinder is nearly zero, indicating the tethering forces are doing their job. However, these flowfields do not yet show vortex formation and shedding at the cylinder. We have not run this code long enough to exhibit these features, which become evident at such a high Reynolds number. In order for the approximate-implicit force calculations to remain stable, we need to use a relatively small time step. This causes the creation of an extremely large number of vortex elements in a small real-time simulation.

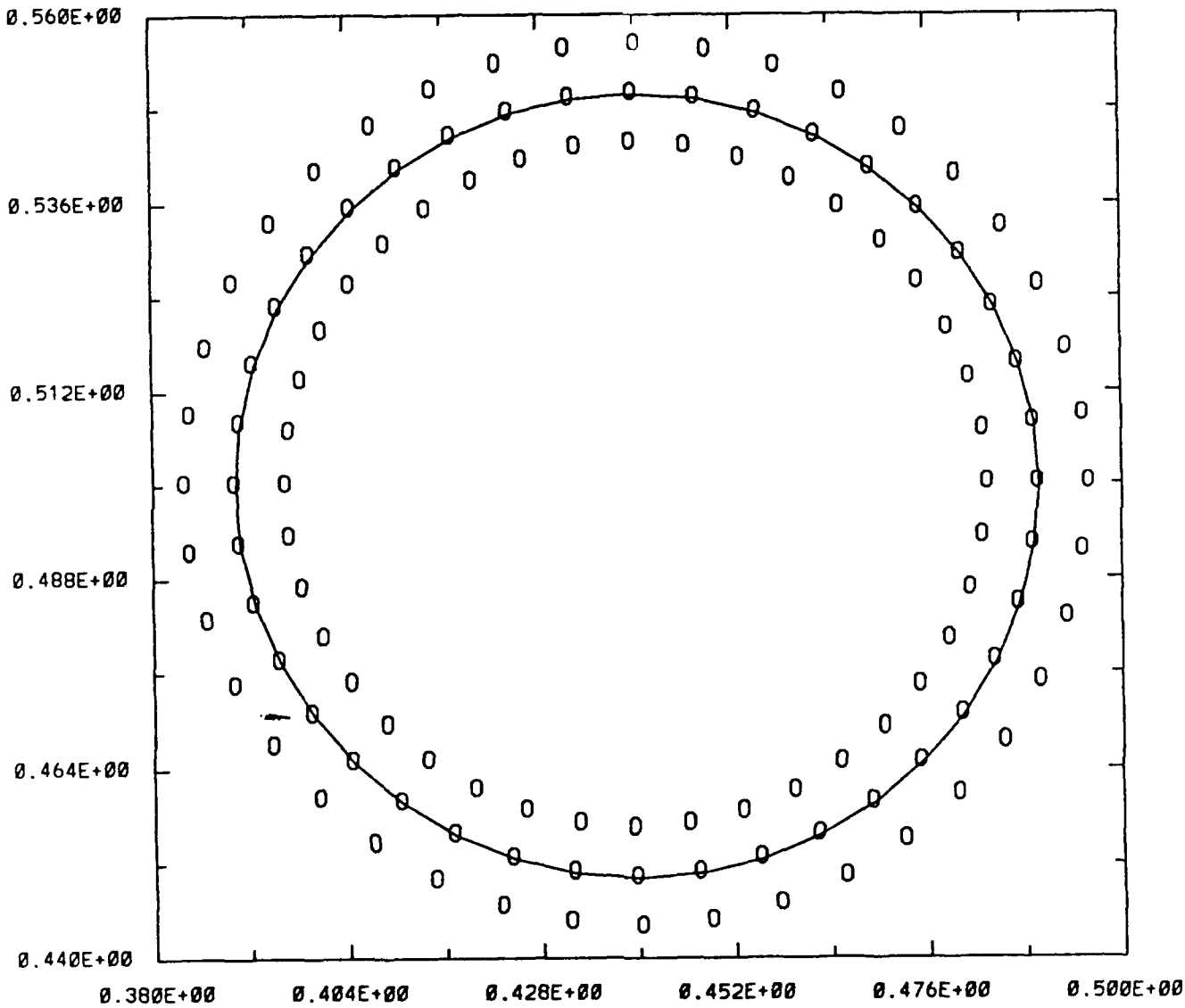

Figure 1. Position of Vortex Elements.

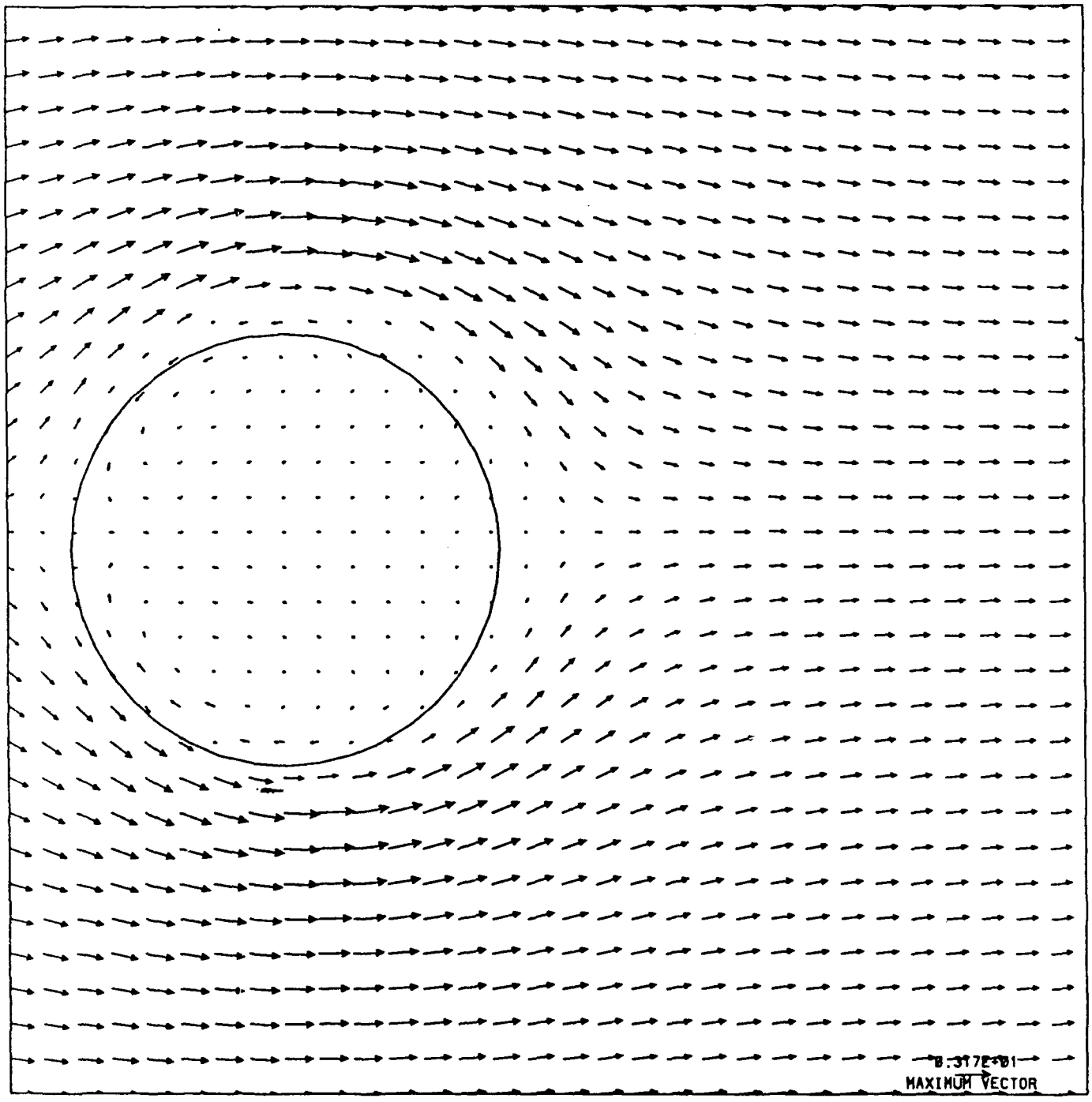

Figure 2. Flow Past Cylinder.

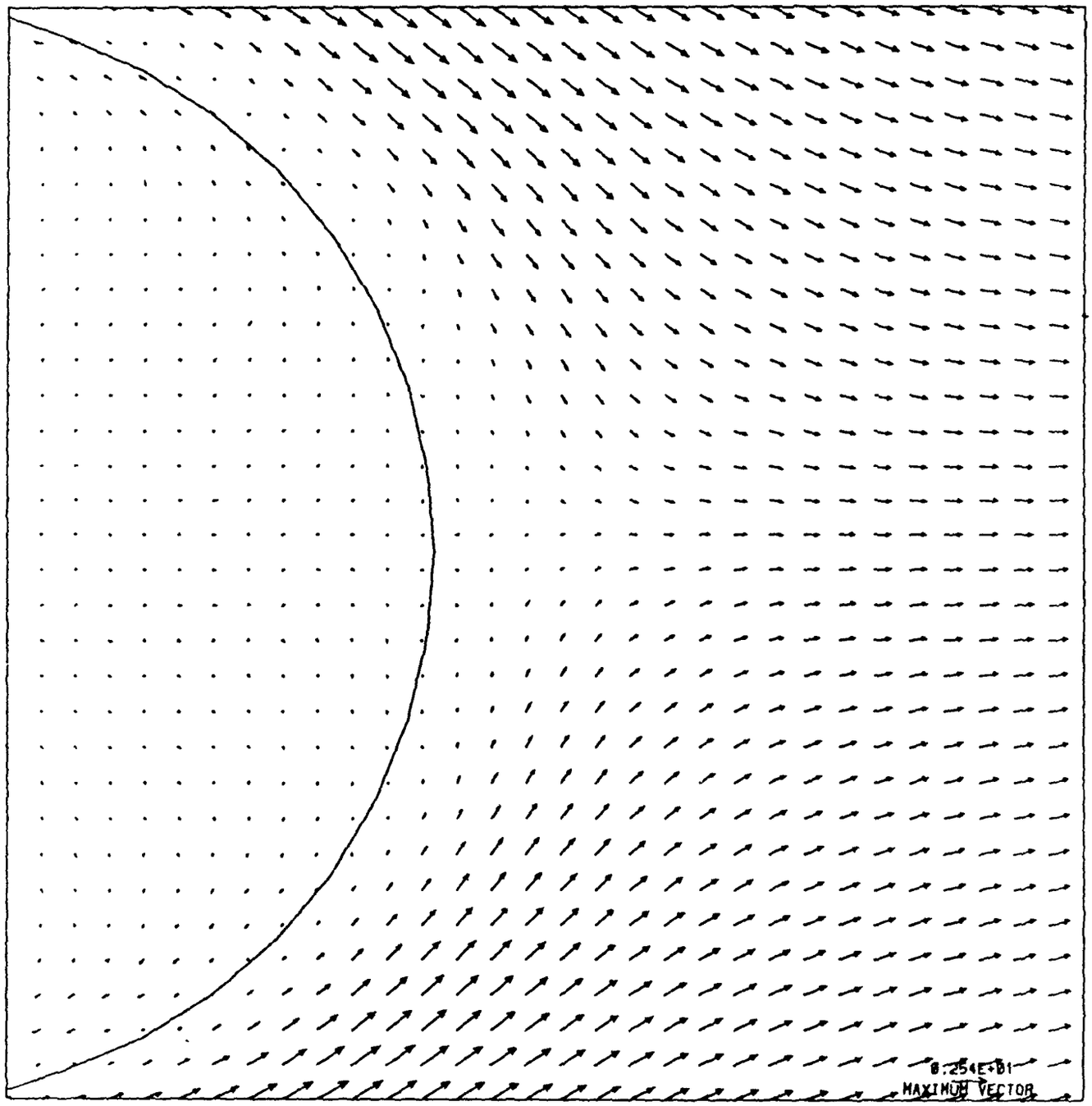

Figure 3. Flow Past Cylinder (Magnified).

Flow Past a Flat Plate

In this example, we will simulate incompressible, inviscid flow about a flat plate which is oriented normal to the free flow. There are 2 possible inviscid flows which are solutions. One is a continuous potential flow which is steady and symmetric with respect to the plate. However, the velocities near the ends of the plate are infinite. Another solution is an unsteady, discontinuous potential flow, which sheds vorticity from the plate [23]. Here, the velocities at the ends of the plate are finite. This solution, when compared with experiments, is more realistic and can be thought of as the vanishing viscosity limit [16].

The flat plate is represented by an elastic boundary which is made up of 40 immersed boundary points. The plate lies on the line $x = 1$ and goes from $y = 1$ to $y = 3$. The plate is tethered to space with springs of resting length zero and stiffness constants 10^7. A uniform background flow of $U = .5$ is imposed. The numerical parameters used are $\Delta t = .001$, $\Delta s = .05$, $h = .4\Delta s$, and $\sigma = .75\Delta s$.

To modify the algorithm to model invisid flow, we discard the random walk which approximates diffusion. Moreover, we only force the *normal* component of velocity of the plate to coincide with that of the fluid. (Our immersed boundary point can therefore only move in the $x-$ direction.) In inviscid flow, tangential slip is allowed.

In these simulations, we are only going to create a single dipole layer of vorticity at the plate (i.e., 2 vortex elements per boundary point are created at each time step). This dipole layer is actually tangent to the plate.

Figure 4 shows velocity fields about the plate at $t = .04, t = .25, t = .5$, and $t = .75$. The first flow field appears to be symmetric about the plate; a wake has not yet had a chance to form. The successive flow fields show the formation of 2 counter-rotating vortices at the ends of the plate. These vortices are getting bigger as time goes on. Our numerical scheme has picked out the unsteady, inviscid solution. We believe this happens because our velocity field, due to the smoothing parameter σ, is not allowed to be infinite anywhere. Moreover, the finiteness of our dipole layer h adds some smearing which is manifested as numerical viscosity.

The dipole layer of vortex elements is initialized to lie tangentially along the plate, except for the 2 elements which are placed a distance of h from the top and the bottom. The vortex elements on the plate move approximately with the same velocities as the tethered boundary points, and thus, approximately remain on the plate. However, vortex elements are shed from the top and bottom. Figure 5 shows the location of vortex elements at time $t = .04$ and at $t = .25$. By $t = .25$ a total of 20,000 vortex elements have been created. Figure 6 shows a contour plot of vorticity at $t = .25$. These figures qualitatively compare to the vortex sheet roll up described in Krasny [16].

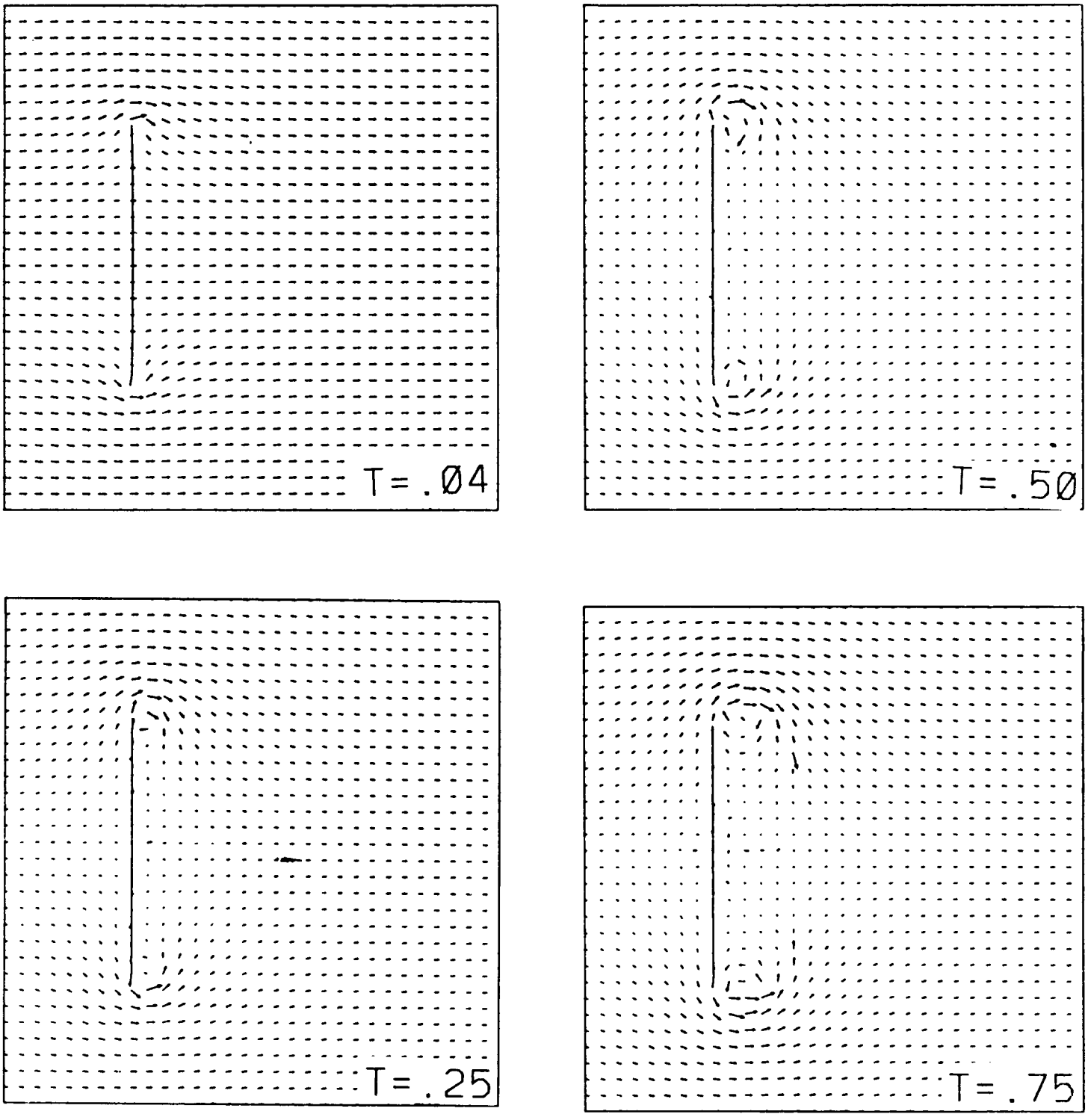

Figure 4. Flow Past Flat Plat .

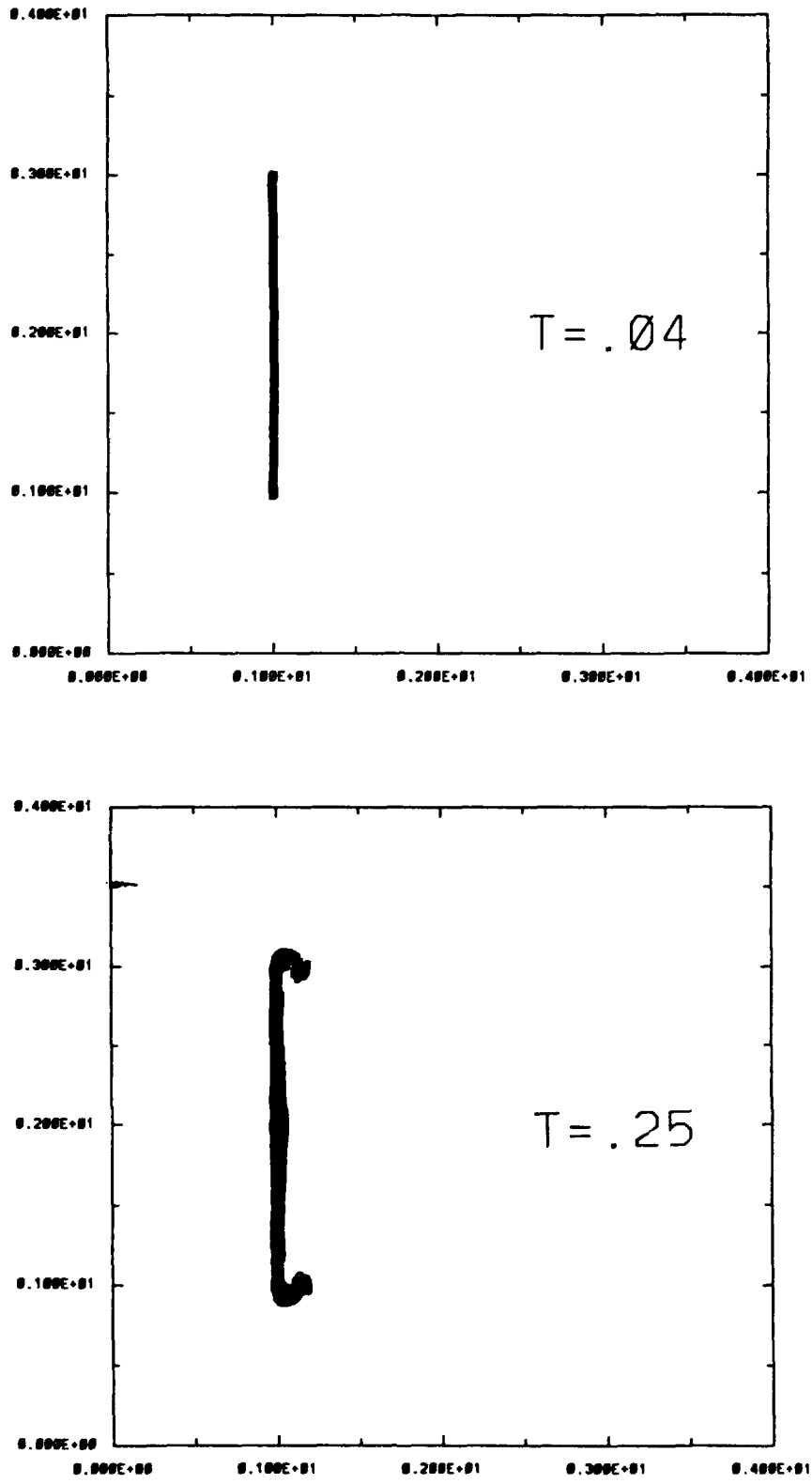

Figure 5. Position of Vortex Elements .

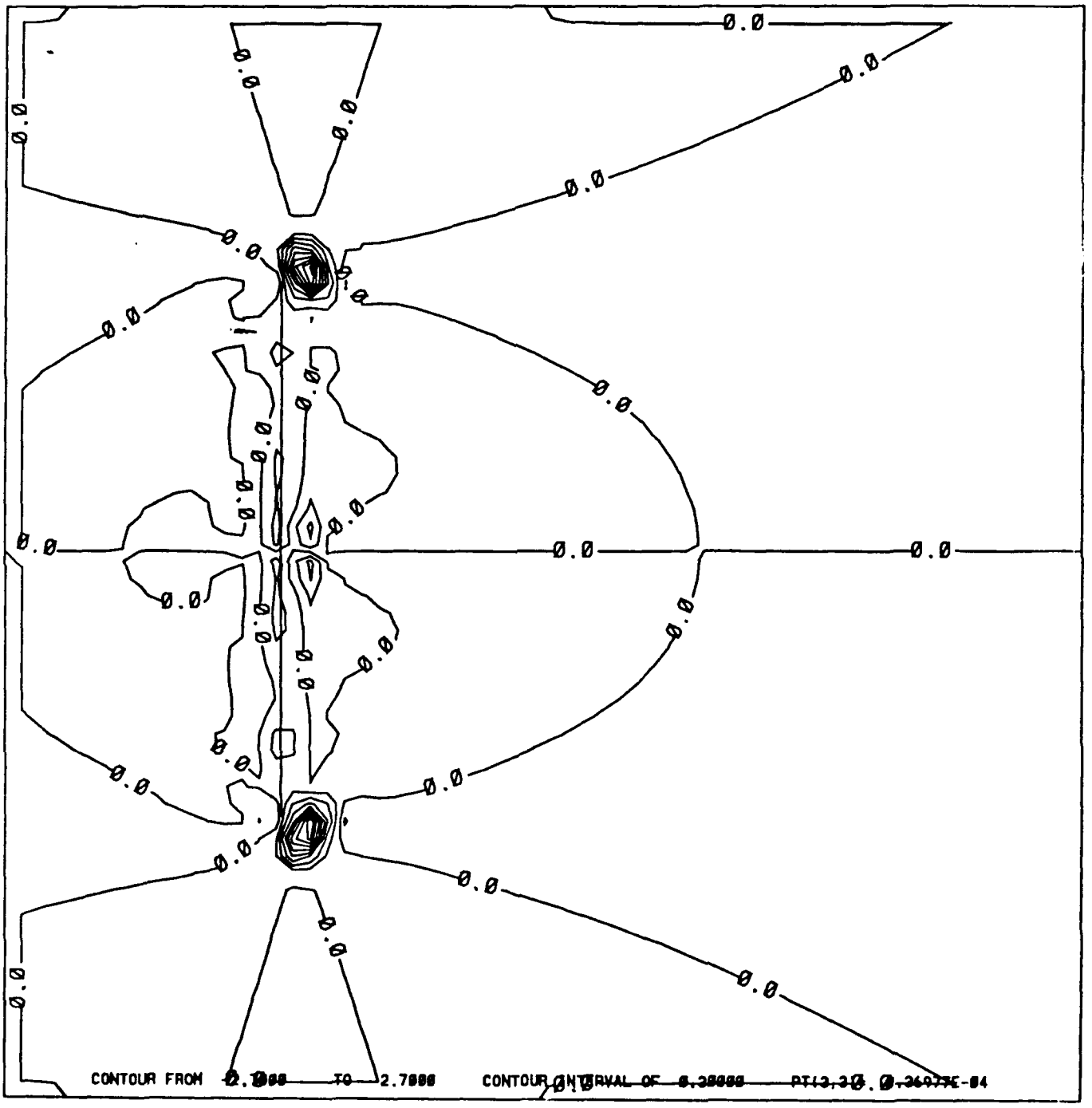

Figure 6. Contours of Vorticity.

CONCLUSIONS AND FUTURE WORK

Finite difference schemes do not perform well in simulations of high Reynolds number flow because a restrictive number of grid points must be used to resolve boundary layers. We have presented a grid-free numerical method which may be used to calculate flows around an immersed elastic boundary. We have presented numerical results in 2 simple cases, where the boundary motion is specified and is not time dependent. Our initial results show that the method gives the correct qualitative features of the desired flow.

The major drawback of this algorithm is the growth of the number of vortex elements at each time step. The computation of the vortex-vortex interactions becomes very expensive. Presently, we are performing the straightforward $O(m_n^2)$ operations, where m_n is the total number of vortex elements present at time step n. There are, however, techniques which can be used to speed up this calculation: Anderson's method of local corrections [1], or the multipole method of Greengard and Rokhlin [13]. We are planning to incorporate one of these techniques in our code.

As the algorithm stands, m_n is always increasing by 2 or 3 times the number of boundary points each time step. In an exterior problem, like flow past a flat plate, we can throw away vortex elements when they move a certain distance from the immersed boundary. However, in interior calculations, like blood flow in the heart, some vortex elements are trapped inside the immersed boundary. We need to investigate the systematic merging of nearby vortex elements in order to make large time simulations feasible.

We need to establish the dependence of this following numerical method on the numerical parameters:

1) The equilibrium distance between boundary points Δs.

2) The small parameter h which determines the distance of the dipole layer from the boundary.

3) The parameter σ used in smoothing the velocity field near the center of the vortex blobs.

We would like to show convergence of this numerical scheme as these parameters are refined. We should also include another parameter, κ_{max} which would be the maximum strength any one vortex element can carry. If a strength $\kappa_i > \kappa_{max}$ is calculated, that vortex element ought to be split up into other elements of smaller strengths, which add up to κ_i. This has shown to be very important in the convergence of standard vortex methods [24].

The numerical examples presented here were chosen for their simplicity. These immersed boundaries do not undergo time dependent motions, and their equilibrium position in space has been specified by specifying tether points. Moreover, each boundary point is uncoupled from its neighbors in the force density calculations. Once a better understanding of the numerical method is achieved on these test problems, we can use it, with very minor modifications, to model time dependent problems in biofluiddynamics.

REFERENCES

[1] Anderson, C. R. A Method of Local Corrections for Computing the Velocity Field Due to a Distribution of Vortex Blobs. J Comp Phys 62:111-123 (1986).

[2] Anderson, C. R. A Vortex Method for Flows with Slight Density Variations. J Comp Phys 61:417-444 (1985).

[3] Bell, J. B., P. Colella and H. M. Glaz. A Second-Order Projection Method for the Incompressible Navier-Stokes Equations. J Comput Phys 85:257-283 (1989).

[4] Beyer, R. P. A Computational Model of the Cochlea using the Immersed Boundary Method. submitted for publication (1990).

[5] Cheer, A. Y. Numerical Study of Incompressible Slightly Viscous Flow Past Blunt Bodies and Airfoils. SIAM J Sci Stat Comp 4:685-705 (1983).

[6] Chorin, A. J. Numerical Solution of the Navier-Stokes Equations. Math Comp 22:745 (1968).

[7] Chorin, A. J. Numerical Study of Slightly Viscous Flows. J Fluid Mech 57:785 (1973).

[8] Fauci, L. J. Interaction of Oscillating Filaments: A Computational Study. J Comput Phys 86:294-313 (1990).

[9] Fauci, L. J. Peristaltic Pumping of Solid Particles. submitted for publication (1991).

[10] Fauci, L. J. and C. S. Peskin, A Computational Model of Aquatic Animal Locomotion. J Comput Phys 77:85-108 (1988).

[11] Fogelson, A. L. A Mathematical Model and Numerical Method for Studying Platelet Adhesion and Aggregation during Blood Clotting. J Comput Phys 56:111-134 (1984).

[12] Ghoniem, A. F. and Y. Cagnon. Vortex Simulation of Laminar Recirculating Flow. J Comp Phys 68:346-377 (1988).

[13] Greengard, L. and V. Rokhlin. A Fast Algorithm for Particle Simulations. J Comp Phys 73:325-348 (1987).

[14] Goodman, J. Convergence of the Random Vortex Method. Comm. Pure Appl Math 40:189-220 (1987).

[15] Krasny, R. Desingularization of Periodic Vortex Sheet Roll-up. J Comp Phys 65:292-313 (1986).

[16] Krasny, R. Vortex Sheet Roll-Up due to the Motion of a Flat Plate. ASME Fed - International Symposium on Nonsteady Fluid Dynamics. 92:449-453 (1990).

[17] McCracken, M. F. and C.S. Peskin. A Vortex Method for Blood Flow through Heart Valves. J Comp Phys 35:183-205 (1980).

[18] Peskin, C. S. Numerical Analysis of Blood Flow in the Heart. J Comp Phys 25:220 (1977).

[19] Peskin, C. S. and D. M. McQueen. A Three-Dimensional Computational Method for Blood Flow in the Heart I. Immersed Elastic Fibers in a Viscous Incompressible Fluid. J Comp Phys 81:372-405 (1989).

[20] Peskin, C. S. and D. M. McQueen. A Three-Dimensional Computational Method for Blood Flow in the Heart II. Contractile Fibers. J Comp Phvs 82:289-297 (1989).

[21] Peskin, C. S. and A. W. Wolfe. The Aortic Sinus Vortex. Federation Proc 37:2785-2792 (1978).

[22] Samn, S. An Advanced Projection Method for Immersed Boundary Problem. in progress(1991).

[23] Sarpkaya, T. An Inviscid Model of Two Dimensional Vortex Shedding for Transient and Asymptotically Steady Separated Flow Over an Inclined Plate. J Fluid Mech 68:109-128 (1975).

[24] Sethian, J. A. and A.F. Ghoniem. Validation Study of Vortex Methods. J Comp Phys 74:283-317 (1988).

* U. S. GOVERNMENT PRINTING OFFICE: 1991--561-052/40063